TASK QUARTERLY 10 No 4, 377–390

MEAN AND TURBULENT THERMAL FIELDS DUE TO FILM COOLING VIA AN EDDY HEAT DIFFUSIVITY CLOSURE

MICHAŁ KARCZ

Institute of Fluid Flow Machinery, Polish Academy of Sciences,
Fiszera 14, 80-952 Gdansk, Poland
mkarcz@imp.gda.pl

(Received 1 September 2006; revised manuscript received 23 September 2006)

Abstract: The two-equation level of turbulent heat flux modelling is considered for application in film cooling instead of the turbulent Prandtl number concept. The investigations involve numerical analysis of mean and fluctuating temperature fields near the coolant injection inlet. The results of the implemented coupled v^2-f-k_θ-ϵ_θ model are compared with measurement data for a flat plate cooled with compound angle orientation of discrete injection holes. The results of numerical analysis agree very well with the experimental data. The coupled model offers a detailed picture of gas turbine cooling problems without using time-consuming, inherently unsteady models.

Keywords: v^2-f-k_θ-ϵ_θ model, turbulent heat flux, temperature fluctuations, film cooling

Nomenclature

$\overline{v}_i$ – mean velocity components, $i = x,y,z$
$\overline{v'^2}$ – wall-normal stress
f – a variable related to the turbulent energy redistribution in the $\overline{v'^2}$ transport equation
k – turbulent kinetic energy
k_θ – temperature variance
Pr_t – turbulent Prandtl number
S_{ij} – strain rate tensor, $i,j = x,y,z$
T – mean temperature
I – momentum flux ratio
M – blowing ratio
VR – velocity ratio

Greeks

α, α_t – molecular and turbulent heat diffusivity
ϵ – dissipation rate of k
ϵ_θ – destruction rate of k_θ
η – film cooling effectiveness
ρ – fluid density
ν, ν_t – molecular and turbulent viscosity
σ_θ – a coefficient for turbulent diffusion of k_θ and ϵ_θ

τ, τ_θ – turbulent velocity and temperature field time scales
θ' – temperature fluctuations

Subscripts
∞ – freestream
c – coolant jet

1. Introduction

The need for cooling highly mechanically and thermally loaded gas turbine elements is obvious. The temperature levels that occur in a modern gas turbine blade path often exceed the melting point of available alloys. There are two common ways to protect gas turbine elements from thermal overload, namely internal and external cooling, shown in Figure 1. Internal cooling consists mainly of ribbed U-ducts located inside the gas turbine blades [1, 2]. External cooling is connected with discrete jets of coolant injected into a hot mainstream by a system of holes [3, 4]. Both cooling systems involve many physical features that are not fully understood and which are still very difficult to model, even with sophisticated closures.

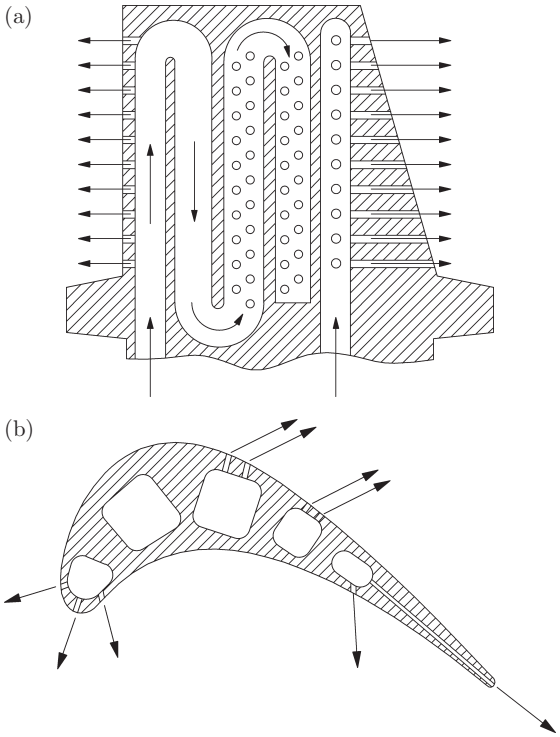

Figure 1. Internal and external cooling systems of a gas turbine blade [5]

Most of the publications concerning external cooling of gas turbines have employed two-equation turbulent momentum flux closures combined with the constant or varying turbulent Prandtl number assumption for turbulent heat flux modelling [6–8]. This approach is very robust but not always effective. A higher level of turbulent heat flux modelling has been considered as a remedy for some of the existing models

deficiences [9–12]. In the framework of eddy diffusivity closure, this means that the two-equation k_θ-ϵ_θ turbulent heat flux model should be adopted. It not only uses a time scale that is characteristic of the turbulent momentum field, but also an additional time scale dedicated to the turbulent thermal field. An alternative coupled v^2-f-k_θ-ϵ_θ model [13] is employed in this study for film cooling analysis. This model is based on Durbin's v^2-f model [2, 14–17] and the two-equation k_θ-ϵ_θ turbulent heat transfer closure of Deng *et al.* [11].

Many experimental and numerical studies have been performed on various film cooling arrangements [3, 4, 6–8]. Most of them have been focused on mean thermal field measurements and predictions with the so-called cooling effectiveness as the main parameters to be investigated. A paper of Gartshore *et al.* [6] is considered as an example, where variously shaped holes are analysed for flat plate cooling purposes. Only a few papers provide information on the turbulent thermal field's behaviour in the immediate vicinity of the coolant jet exit. Among these the experimental results of Kohli and Bogard [4] appear to be the most interesting for the k_θ-ϵ_θ type of closure validation.

2. The v^2-f-k_θ-ϵ_θ model

Turbulence effects are usually taken into account using an eddy diffusivity concept. Then the constitutive closures of turbulent momentum and heat fluxes are as follows [14]:

$$-\overline{v_i' v_j'} = 2\nu_t \left(S_{ij} - \frac{1}{3}\frac{\partial \overline{v}_k}{\partial x_k}\delta_{ij} \right) - \frac{2}{3}k\delta_{ij}, \tag{1}$$

$$-\overline{v_j' \theta'} = \alpha_t \frac{\partial T}{\partial x_j}. \tag{2}$$

Turbulent heat flux computations are usually simplified by introducing the so-called Reynolds analogy, which directly links turbulent diffusivity of heat, α_t, with turbulent viscosity, ν_t, with the turbulent Prandtl number, Pr_t [18]:

$$\mathrm{Pr}_t = \frac{\nu_t}{\alpha_t}. \tag{3}$$

Employing a constant value of Pr_t close to unity or using a Kays-Crawford formula for Pr_t estimation [16, 18] yields quite satisfactory results for near-wall flows. The eddy diffusivity of heat should nevertheless be represented as a function of turbulent time scales for velocity and temperature fields. It is the main assumption of the two-equation k_θ-ϵ_θ level of turbulent heat flux modelling [10–12].

The derivation of the coupled v^2-f-k_θ-ϵ_θ model can be found in papers [19, 13]. It rests on the assumption that both turbulent momentum and heat transfer are determined by the velocity fluctuations normal to the wall, $\overline{v'^2}$ [15]. In fact, variations of $\overline{v'^2}$ in the close vicinity of the wall govern the wall-friction and heat transfer coefficients [9].

In an analogy to the eddy viscosity formula of the v^2-f model, in the following form:

$$\nu_t = C_\mu \overline{v'^2} \tau, \tag{4}$$

eddy heat diffusivity has been proposed as [19, 13]:

$$\alpha_t = C_\lambda \overline{v'^2} \tau_m. \tag{5}$$

When formula (5) is employed, a mixed time scale, τ_m, is used which includes the dynamic time scale, τ, and the thermal field time scale, τ_θ:

$$\alpha_t = C_\lambda \overline{v'^2} \left(\frac{k}{\epsilon}\right)^l \left(\frac{k_\theta}{\epsilon_\theta}\right)^m, \qquad l+m=1. \tag{6}$$

The dynamic or turbulent time scale of a velocity field, τ, is usually defined as a ratio of turbulent kinetic energy, k, and its dissipation rate, ϵ. The turbulent thermal field time scale, τ_θ, is a ratio of the fluctuating temperature variance, k_θ, and its destruction rate, ϵ_θ. At the same time, when the standard turbulent Prandtl number assumption is employed, only the time scale of the fluctuating velocity field, τ, governs both turbulent momentum and heat transfer.

2.1. Model of the velocity field

Various complex flows have been successfully investigated with the aid of Durbin's v^2-f model: a ribbed duct [2], impinging jets [16], blade passages [14], cooled blades [7], *etc.* In all cases, the v^2-f model appeared to be superior to the known two-equation models, thanks to an introduction of elliptic relaxation to represent non-local effects in near-wall turbulences [15].

The full set of governing equations of the v^2-f model is as follows [2, 13, 16, 19]:

$$\frac{Dk}{Dt} = \frac{\partial}{\partial x_j}\left[\left(\nu + \frac{\nu_t}{\sigma_k}\right)\frac{\partial k}{\partial x_j}\right] + P_k - \epsilon, \tag{7}$$

$$\frac{D\epsilon}{Dt} = \frac{\partial}{\partial x_j}\left[\left(\nu + \frac{\nu_t}{\sigma_\epsilon}\right)\frac{\partial \epsilon}{\partial x_j}\right] + \frac{C_{\epsilon 1}P_k - C_{\epsilon 2}\epsilon}{\tau}, \tag{8}$$

$$\frac{D\overline{v'^2}}{Dt} = \frac{\partial}{\partial x_j}\left[(\nu + \nu_t)\frac{\partial \overline{v'^2}}{\partial x_j}\right] + kf - \frac{\epsilon}{k}\overline{v'^2}, \tag{9}$$

$$f = L^2 \frac{\partial}{\partial x_j}\left(\frac{\partial f}{\partial x_j}\right) + \frac{C_1}{\tau}\left[\frac{2}{3} - \frac{\overline{v'^2}}{k}\right] + C_2\frac{P_k}{k}. \tag{10}$$

Turbulent viscosity, ν_t, is defined with formula (4). The production of turbulent kinetic energy, P_k, is given by:

$$P_k = 2\nu_t S_{ij} S_{ij}, \tag{11}$$

where S_{ij} is the strain-rate tensor defined as:

$$S_{ij} = \frac{1}{2}\left(\frac{\partial \overline{v}_i}{\partial x_j} + \frac{\partial \overline{v}_j}{\partial x_i}\right). \tag{12}$$

The time and length scales which appear in Equations (8) and (10) are as follows:

$$\tau = \max\left[\frac{k}{\epsilon}, 6\sqrt{\frac{\nu}{\epsilon}}\right] \tag{13}$$

and

$$L = C_L \max\left[\frac{k^{3/2}}{\epsilon}, C_\eta\left(\frac{\nu^3}{\epsilon}\right)^{\frac{1}{4}}\right]. \tag{14}$$

Following the paper of Sveningsson and Davidson [17], any time scales bounding as in [2, 7, 14, 16] are excluded from the model. Instead of these only bound on the eddy viscosity (4), in the form proposed in [17], is employed:

$$\nu_t = \min\left[\nu_t, \frac{0.6k}{\sqrt{6S_{ij}S_{ij}}}\right]. \tag{15}$$

Such bounding prevents spurious growth of turbulence kinetic energy under large rates of strain in the vicinity of stagnation points.

The v^2-f model constants employed in the present analysis are the same as those of [2, 13]:

$$\begin{aligned} &C_\mu = 0.22, \quad C_1 = 0.4, \quad C_2 = 0.3, \quad C_L = 0.25, \\ &C_\eta = 85, \quad C_{\epsilon 2} = 1.9, \quad \sigma_\epsilon = 1.3, \\ &C_{\epsilon 1} = 1.4\left(1 + 0045\sqrt{k/\overline{v'^2}}\right). \end{aligned} \tag{16}$$

The boundary conditions for solid walls ($y \to 0$) are:

$$k = 0, \quad \epsilon \to \frac{2\nu k}{y^2}, \quad \overline{v'^2} = 0, \quad f \to -\frac{20\nu^2\overline{v'^2}}{\epsilon y^4}. \tag{17}$$

2.2. Model of the thermal field

A two-equation closure of turbulent heat flux was successfully implemented by Nagano and Kim [10], followed by other versions of the k_θ-ϵ_θ model [11, 12]. The presented v^2-f-k_θ-ϵ_θ model is partly based on the assumptions given in [11, 12]. The full set of governing equations for temperature variance and its destruction rate, in the framework of the coupled model, is as follows [13]:

$$\frac{Dk_\theta}{Dt} = \frac{\partial}{\partial x_j}\left[\left(\alpha + \frac{\alpha_t}{\sigma_\theta}\right)\frac{\partial k_\theta}{\partial x_j}\right] + P_\theta - \epsilon_\theta, \tag{18}$$

$$\begin{aligned} \frac{D\epsilon_\theta}{Dt} = &\frac{\partial}{\partial x_j}\left[\left(\alpha + \frac{\alpha_t}{\sigma_\theta}\right)\frac{\partial \epsilon_\theta}{\partial x_j}\right] + C_{p1}\overline{v'^2}\left(\frac{\partial T}{\partial x_j}\right)^2 \\ &- C_{d1}\epsilon_\theta\frac{\epsilon_\theta}{k_\theta} - C_{d2}\epsilon_\theta\frac{\epsilon}{k}. \end{aligned} \tag{19}$$

The P_θ production term is modelled with the following equation:

$$P_\theta = \alpha_t\frac{\partial T}{\partial x_j}\frac{\partial T}{\partial x_j}. \tag{20}$$

The eddy diffusivity of heat, α_t, is given by formula (5). Following Deng *et al.*'s proposition, a single production term is included in the transport Equation (19) of the coupled model. The term is responsible for approximation of all the generation sources of ϵ_θ [13] .

The constants of the implemented two-equation model have been assumed as follows [13]:

$$C_\lambda = 0.2, \quad C_{p1} = 2.0, \quad C_{d1} = 1.0, \quad C_{d2} = 0.9,$$
$$l = 1.5, \quad m = -0.5, \quad \sigma_\theta = 1.0. \tag{21}$$

The boundary conditions on the impermeable walls have been assumed to be identical to other two-equation heat flux closures [11, 12]:

$$k_\theta = 0, \quad \epsilon_\theta \to \alpha \frac{k_\theta}{y^2}. \tag{22}$$

3. Computational results

The coupled model [19, 13] has been validated in two different experiments involving flat plate cooling. The experiment of Gartshore *et al.* [6] has provided results for flat plate cooling with variously shaped holes for three different values of the velocity ratio, VR. At the same time, the measurements of Kohli and Bogard [4] offer a unique possibility to compare not only mean but also fluctuating thermal fields with the numerical predictions.

3.1. The flow configuration

Both analysed experiments involved a flat plate and film cooling. Their geometrical configuration was typical, as shown in Figure 2.

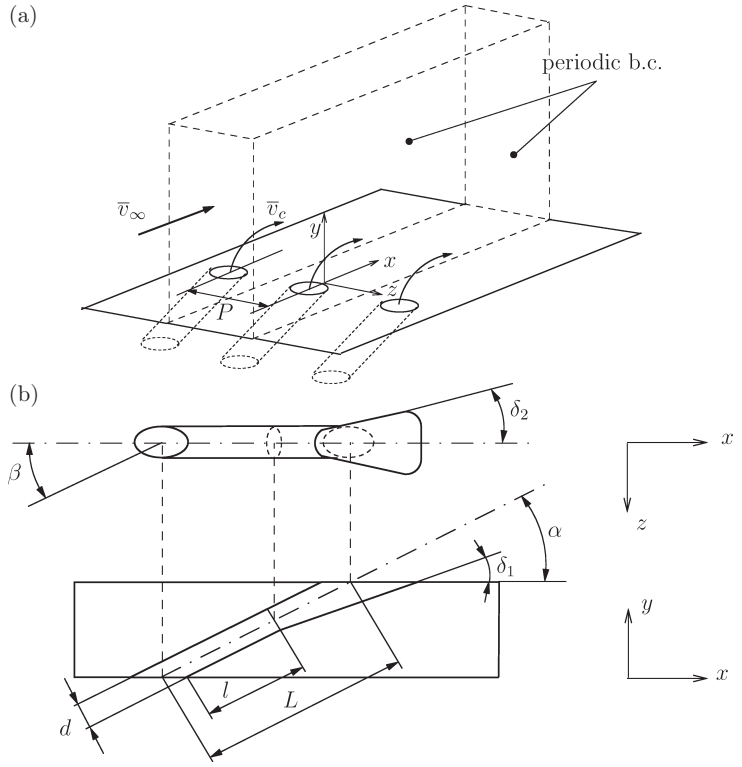

Figure 2. Typical geometrical parameters of flat plate film cooling arrangements: (a) general configuration of a cooling plate with discrete holes, (b) detailed geometry of a hole in a plate's cross-section

The experiment of Gartshore *et al.* [6] was performed for two differently shaped holes – one round $d = 14.4$mm, the other square $d = 12.7$mm – of the same angles and aspect ratios typical for real gas turbine configuration, *viz.* $P/d = 3$, $L/d = 4$, inclination angle $\alpha = 30^{\circ}$, lateral angle $\beta = 45^{\circ}$ and the angle of flaring of holes near the exit $\delta_1 = \delta_2 = 0^{\circ}$, as per Figure 2. Various velocity ratios of the coolant jet to the mainstream, $\overline{v}_c/\overline{v}_\infty$, were considered, VR = 0.5, 1.0 and 1.5. The measurements were performed for the low free-stream turbulence level ranging from Tu = 1% for VR = 0.5 to Tu = 3% for VR = 1.5.

The results of Kohli and Bogard's measurements [4] were obtained for a similar configuration with $d = 11.11$mm, $P/d = 3$, $L/d = 4$, inclination angle $\alpha = 35^{\circ}$, lateral angle $\beta = 0^{\circ}$ and $\delta_1 = \delta_2 = 0^{\circ}$. Their measurements were conducted for a momentum flux ratio $(\rho_c \overline{v}_c^2)/(\rho_\infty \overline{v}_\infty^2)$ of the coolant jet to the mainstream of $I = 0.16$, with the corresponding blowing or mass flux ratio $(\rho_c \overline{v}_c)/(\rho_\infty \overline{v}_\infty)$ of $M = 0.40$ and the velocity ratio of VR = 0.38. The free-stream velocity was fixed at $\overline{v}_\infty = 10$ m/s and the inlet turbulence level was assumed to equal Tu = 0.5%. The inlet temperature difference between the mainstream and the jet was 15 K.

For numerical purposes, only a part of the flat plate with a single hole was investigated with periodic boundary conditions imposed in the spanwise direction, as shown in Figure 2.

3.2. The numerical procedure

A commercial CFD code, FLUENT 6.2.18 [20], based on the finite volume method was used to solve the sets of Equations (7)–(10) for the turbulent momentum field and Equations (18)–(19) for the turbulent thermal field, together with mean continuity, momentum and energy equations.

The six differential equations of the coupled model were implemented into the solver by an external subroutine [13, 19]. The second-order scheme was employed to discretize convection terms of the mean momentum balance, energy balance and the scalar evolution equations. The diffusion terms for all of equations were central-differenced. The SIMPLE method was used for pressure-velocity coupling.

For both computational cases, structural and hexahedral multiblock grids were built and tested with exponential near-wall refinement. For the first case, based on the Gartshore *et al.* experiment, the total number of finite volumes was equal to 241 310 cells for a round-shaped hole and 219 600 for a square one. For the Kohli and Bogard experiment, 257 025 cells were employed, sufficient for a v^2-f computation. The number of cells was determined on the basis of the grid sensitivity studies.

The boundary conditions were related to appropriated experimental data. Full turbulent flow was assumed at the mainstream inlets, with the k and ϵ profiles estimated from the experimental turbulence level, Tu.

3.3. Flat plate cooling via round and square shaped holes

The most common way to analyse the film cooling effects is to investigate spatial distribution of film cooling effectiveness, η. The dimensionless cooling effectiveness, or normalised temperature, is defined to be [3, 4, 6, 8]:

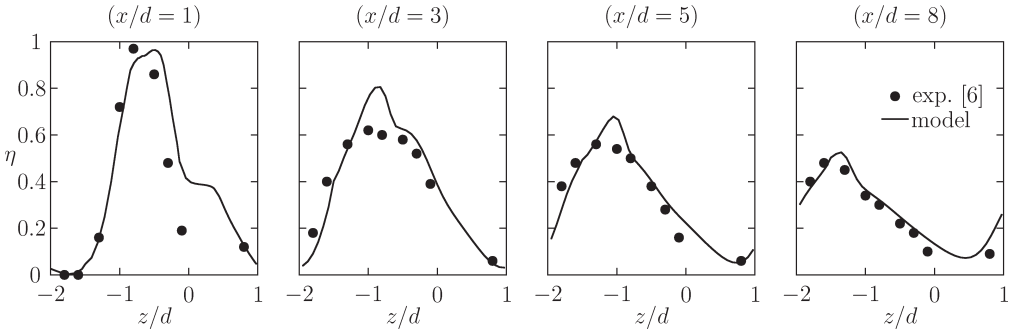

Figure 3. Cooling effectiveness, η, for round shaped holes (VR = 0.5)

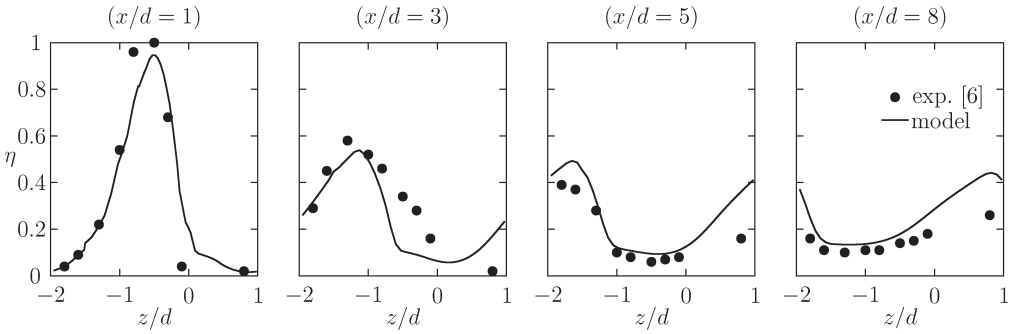

Figure 4. Cooling effectiveness, η, for round shaped holes (VR = 1.0)

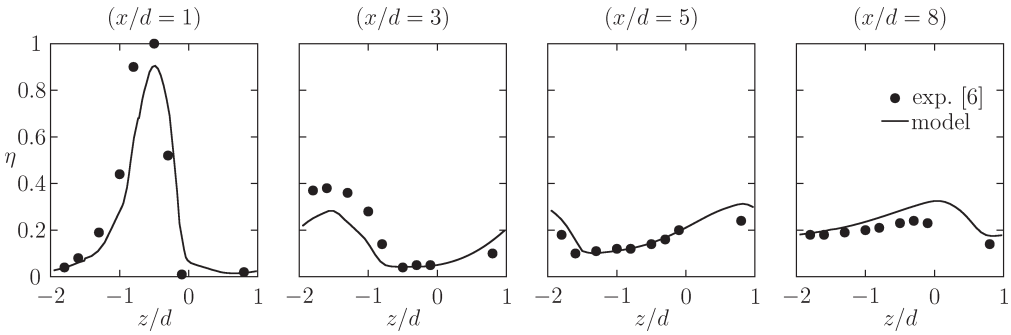

Figure 5. Cooling effectiveness, η, for round shaped holes (VR = 1.5)

$$\eta = \frac{T - T_\infty}{T_c - T_\infty}, \tag{23}$$

where T represents local static temperature, T_c is the temperature of the coolant jet and T_∞ describes the mainstream temperature.

The results of spanwise distribution of the η coefficient for velocity ratios VR = 0.5, 1.0 and 1.5 will be presented in diagrams below, for four locations of duct cross-sections from the cooling hole outlet, namely $x/d = 1$, 3, 5 and 8. The numerical predictions are compared with the Gartshore *et al.* data [6].

The results for the velocity ratio of VR = 0.5 for round-shaped holes are presented in Figure 3. Good agreement can be observed between the computational and the experimental data. Especially far from the hole exit, at the distances of

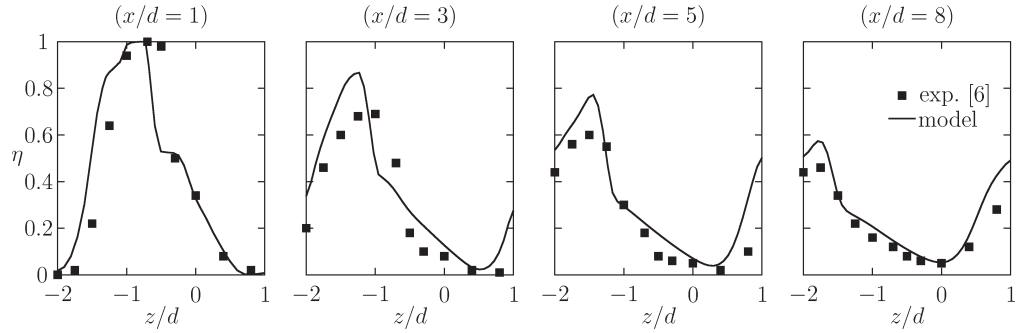

Figure 6. Cooling effectiveness, η, for square shaped holes (VR = 0.5)

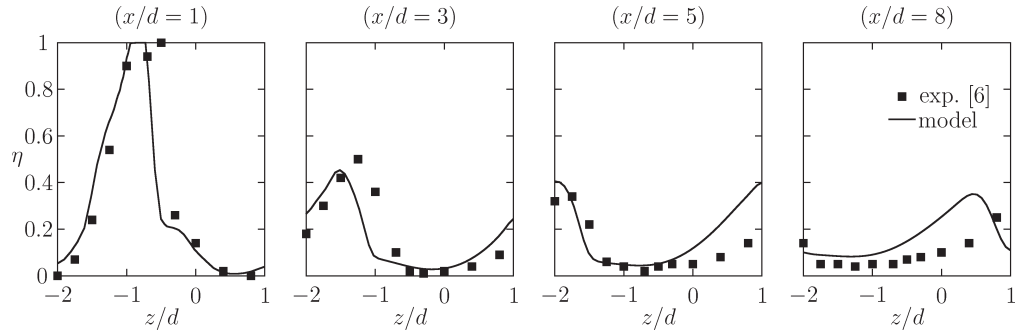

Figure 7. Cooling effectiveness, η, for square shaped holes (VR = 1.0)

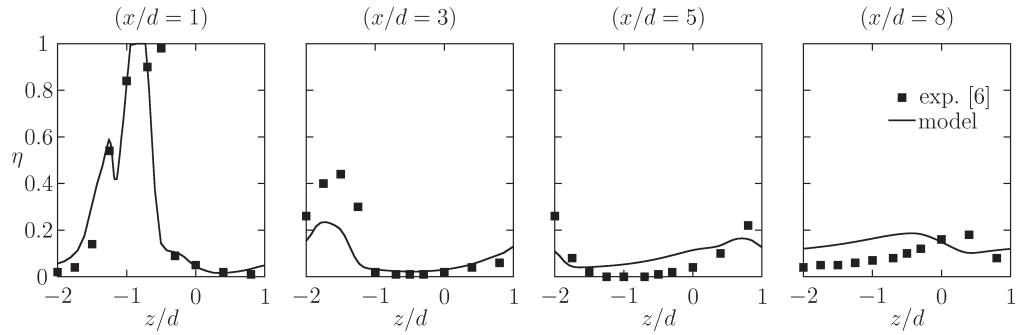

Figure 8. Cooling effectiveness, η, for square shaped holes (VR = 1.5)

$x/d = 5$ and 8, the numerical results of the v^2-f-k_θ-ϵ_θ model show particularly good agreement with the measurements.

Similar conclusions can be drawn for the velocity ratios VR = 1.0 and VR = 1.5 presented in Figures 4 and 5, respectively. For all cases, the discrepancies are clearly visible for the $x/d = 3$ cross-section, where the η coefficient is overpredicted for VR = 0.5 and slightly underestimated at elevated velocity ratios.

Results obtained for square shaped holes are quite similar to those for round ones. The best agreement has been obtained for the lowest VR = 0.5 (see Figure 6), especially away from the hole exit. For the higher velocity ratios, *i.e.* VR = 1.0 and VR = 1.5 as respectively shown in Figures 7 and 8, the quantitative agreement with experimental data is worse as square-shaped holes generate more complex flow

structures that are difficult to capture. At the same time, numerical predictions for all the cases correlate quite well with the Gartshore *et al.* measurements [6].

3.4. Fluctuating thermal field near the hole exit

The experimental data of Kohli and Bogard [4] allow us to compare contours of the cooling effectiveness coefficient, η, and the normalized rms temperature fluctuations, θ'_{rms}, at various spanwise cross-sections, $x/d = -0.5$, 1.0, 3.0, and in the streamwise direction in the jet centre plane $z/d = 0$. The cooling effectiveness coefficient has been defined above with formula (23). The values of θ'_{rms} are obtained directly from the temperature variance equation, remembering that $k_\theta = \overline{\theta'^2}/2$, by proper normalization:

$$\theta'_{\mathrm{rms}} = \frac{\sqrt{\overline{\theta'^2}}}{(T_c - T_\infty)}. \tag{24}$$

The mean thermal fields in the form of the cooling effectiveness coefficient are presented in Figures 9 and 10.

Unlike in the experiment, the modelled coolant jet is not attached to the wall after injection but lifts off slightly. The core of the coolant flow is clearly visible in Figure 10; the contours are symmetrical and the coolant jet maintains its shape relatively far from the hole exit, $x/d = 3$. At the same time, the level of cooling effectiveness, η, has been predicted quite well. The computed cooling effectiveness distributions correlate very well with experimental data in streamwise x/d and spanwise z/d directions.

Similar conclusions can be drawn for turbulent thermal fields, with even better qualitative and quantitative agreement. The contour of the root-mean-square temperature fluctuation, θ'_{rms}, in the vicinity of the cooling air injection hole is presented in Figure 11. The highest level of temperature fluctuations can be observed in the region of the cooling hole's leading edge and far at the interface between the coolant jet and the mainstream, where the velocity and temperature gradients are the greatest, and the turbulent mixing processes are the most intensive.

The maximum observed value of temperature fluctuations is $\theta'_{\mathrm{rms}} = 0.22$. It is close to the experimental data presented by Kohli *et al.* [4], where the measured level of temperature fluctuations was estimated as high as $\theta'_{\mathrm{rms}} \geq 0.25$, which indicated strong fluctuations in the temperature field. Localizations of the maximum θ'_{rms} are

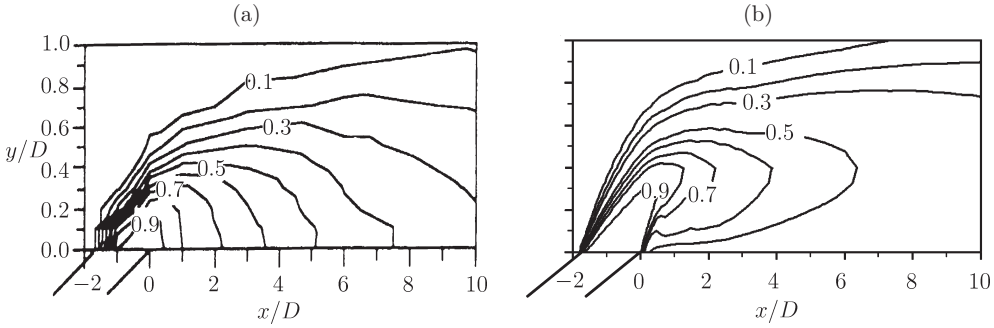

Figure 9. Cooling effectiveness, η, at the jet centre plane: (a) experimental data [4], (b) the v^2-f-k_θ-ϵ_θ model

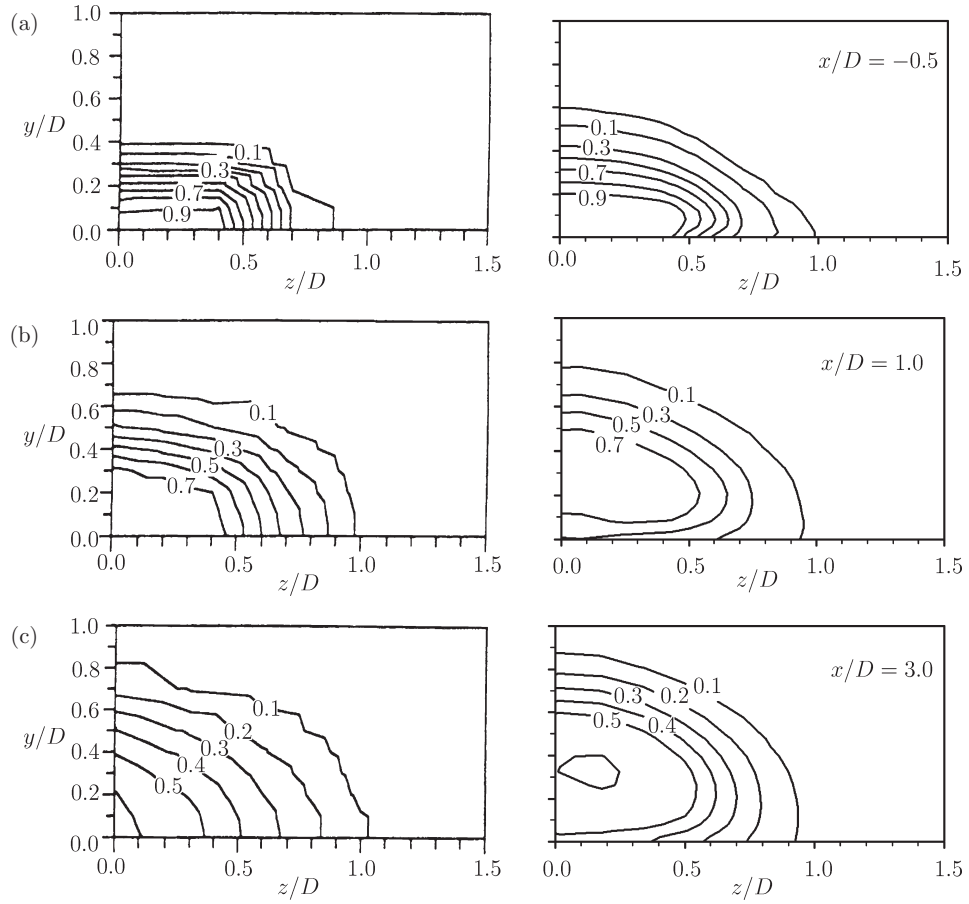

Figure 10. Lateral cooling effectiveness, η, contours at various streamwise positions: (a) $x/D = -0.5$, (b) $x/D = 1.0$, (c) $x/d = 1.5$ (the left column shows experimental data from [4], the right column – the present results for the v^2-f-k_θ-ϵ_θ model)

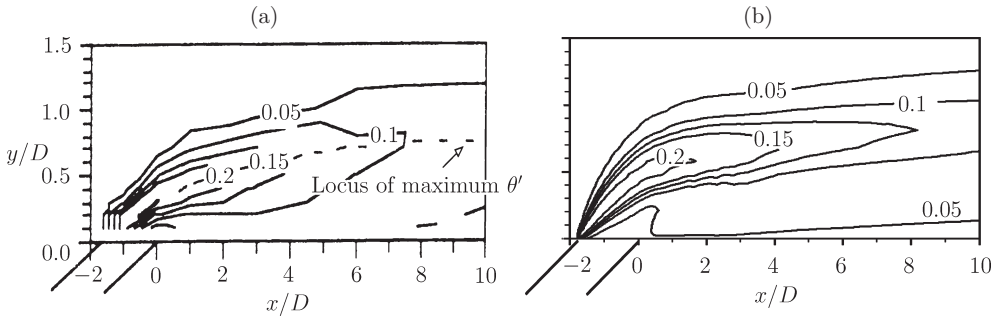

Figure 11. Temperature fluctuations, $\theta'_{\rm rms}$, at the jet centre plane: (a) experimental data [4], (b) the v^2-f-k_θ-ϵ_θ model

almost identical. In the spanwise direction (see Figure 12), only the vertical range of $\theta'_{\rm rms}$ isolines is slightly overestimated.

The strong interactions at the interface between the cooling jet and the mainstream shown in Figures 11 and 12 can be explained by instability of the shear

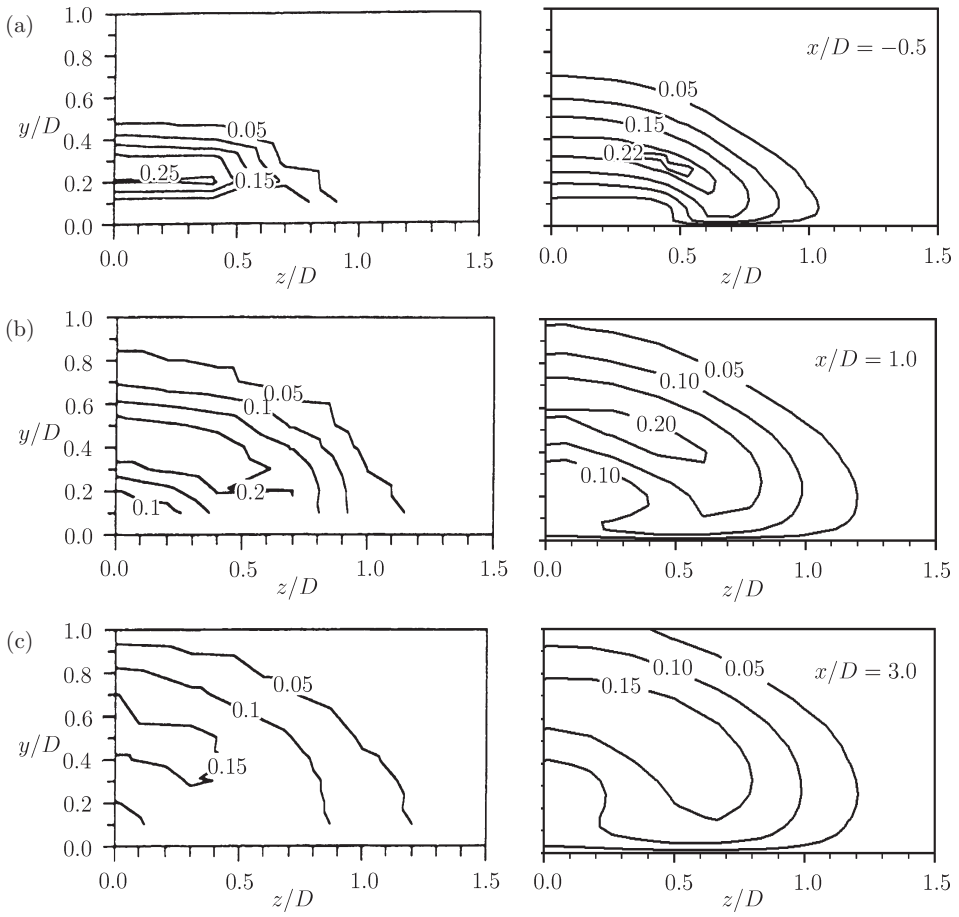

Figure 12. Lateral temperature fluctuation, $\theta'_{\rm rms}$, contours at various streamwise positions: (a) $x/D=-0.5$, (b) $x/D=1.0$, (c) $x/d=1.5$ (the left column shows experimental data from [4], the right column – the present results for the v^2-f-k_θ-ϵ_θ model)

layer that generates large-scale eddy structures [4]. These structures are responsible for the rapid dilution of the coolant jet by the hot mainstream in the case of low free-stream turbulence level. The rapid drop of cooling effectiveness is then observed close to the injection hole: coefficient η loses over half of its value by $x/D=5$, as per Figures 9 and 10. This problem was discussed by Kohli and Bogard [4] and in Lakehal *et al.* [8].

4. Conclusions

Two-equation eddy heat diffusivity closures based on the temperature variation, k_θ, and its destruction rate, ϵ_θ, transport equations, have become a reliable alternative to the standard constant or varying turbulent Prandtl number concept. So far, such closures have been employed only for relatively simple flows in channels, pipes or over backward-facing steps [11–13, 19], due to the inability of the existing low-Re-number models for turbulent momentum transport to cope with more complex flows.

The v^2-f model is known to produce better results than most of the low-Re-number closures, especially for separation flows and flows with a favourable pressure gradient [2, 7, 14–17]. The coupled v^2-f-k_θ-ϵ_θ model can be successfully adopted in the case of mixing the coolant jet and the hot mainstream, as in film cooling arrangements. Some disadvantages due to increasing the computational time, by employing two transport equations for eddy heat diffusivity estimation are recompensed for by additional insights into the flow structure.

The coupled model predicts very well the mean thermal fields of various film cooling configurations and for a wide range of flow parameters. The results concern the distribution of normalized temperature fluctuations, θ'_{rms}, calculated on the basis of the temperature variance Equation (18), are very encouraging. Good agreement has been achieved with the experimental results of Kohli *et al.* [4], both in the level of θ'_{rms} and its spatial distribution.

References

[1] Iacovides H and Launder B E 1995 *Computational fluid dynamics applied to internal gas-turbine blade cooling: a review*, *Int. J. Heat Fluid Flow* **16** 454

[2] Manceau R, Parneix S and Laurence D 2000 *Turbulent heat transfer predictions using the $\overline{v^2}$–f model on unstructured meshes*, *Int. J. Heat Fluid Flow* **21** 320

[3] Kim Y J and Kim S M 2004 *Influence of shaped injection holes on turbine blade leading edge film cooling*, *Int. J. Heat Mass Transfer* **47** 245

[4] Kohli A and Bogard D G 1998 *Fluctuating thermal field in the near-hole region for film cooling flows*, *ASME J. Turbomachinery* **120** 86

[5] Chmielniak T, Rusin A and Czwiertnia K 2001 *Gas Turbines*, Zakład Narodowy im. Ossolińskich, Wroclaw (in Polish)

[6] Gartshore I, Salcudean M and Hassan I 2001 *Film cooling injection hole geometry: Hole shape comparison for compound cooling orientation*, *AIAA J.* **39** 1493

[7] Medic G and Durbin P A 2002 *Toward improved film cooling prediction*, *ASME J. Turbomachinery* **124** 193

[8] Lakehal D, Theodoridis G S and Rodi W 1998 *Computation of film cooling of a flat plate by lateral injection from a row of holes*, *Int. J. Heat Fluid Flow* **19** 418

[9] Launder B E 1988 *On the computation of convective heat transfer in complex turbulent flows*, *ASME J. Heat Transfer* **110** 1112

[10] Nagano Y and Kim C 1988 *A two-equation model for heat transport in wall turbulent shear flows*, *ASME J. Heat Transfer* **110** 583

[11] Deng B, Wu W and Xi S 2001 *A near-wall two-equation heat transfer model for wall turbulent flows*, *Int. J. Heat Mass Transfer* **44** 691

[12] Shikazono N and Kasagi N 1996 *Second–moment closure for turbulent scalar transport at various Prandtl numbers*, *Int. J. Heat Mass Transfer* **39** 2977

[13] Karcz M and Badur J 2005 *An alternative two-equation turbulent heat diffusivity closure*, *Int. J. Heat Mass Transfer* **48** 2013

[14] Medic G and Durbin P A 2002 *Toward improved prediction of heat transfer on turbine blades*, *ASME J. Turbomachinery* **124** 187

[15] Durbin P A 1993 *Application of near-wall turbulence model to boundary layers and heat transfer*, *Int. J. Heat Fluid Flow* **14** 316

[16] Behnia M, Parneix S, Shabany Y and Durbin P A 1999 *Numerical study of turbulent heat transfer in confined and unconfined impinging jets*, *Int. J. Heat Fluid Flow* **23** 1

[17] Sveningsson A and Davidson L 2004 *Assessment of realizability constraints in $\overline{v^2} - f$ turbulence models*, *Int. J. Heat Fluid Flow* **23** 785

[18] Kays W M 1994 *Turbulent Prandtl number – Where are we?*, *ASME J. Heat Transfer* **116** 284

[19] Karcz M and Badur J 2003 *A turbulent heat flux two-equation $\overline{\theta'^2} - \epsilon_\theta$ closure based on the V2F turbulence model*, *TASK Quart.* **7** 375
[20] 2005 *Fluent User's Guide*, Fluent Inc., Lebanon, USA